Ferromagnetism in Narrow Bands of Moiré Superlattices

Cécile Repellin[®], Zhihuan Dong, Ya-Hui Zhang, and T. Senthil Department of Physics, Massachusetts Institute of Technology, Cambridge, Massachusetts 02139, USA

(Received 6 August 2019; revised manuscript received 27 January 2020; accepted 20 April 2020; published 7 May 2020)

Many graphene moiré superlattices host narrow bands with nonzero valley Chern numbers. We provide analytical and numerical evidence for a robust spin and/or valley polarized insulator at total integer band filling in nearly flat bands of several different moiré materials. In the limit of a perfectly flat band, we present analytical arguments in favor of the ferromagnetic state substantiated by numerical calculations. Further, we numerically evaluate its stability for a finite bandwidth. We provide exact diagonalization results for models appropriate for ABC trilayer graphene aligned with hBN, twisted double bilayer graphene, and twisted bilayer graphene aligned with hBN. We also provide DMRG results for a honeycomb lattice with a quasiflat band and nonzero Chern number, which extend our results to larger system sizes. We find a maximally spin and valley polarized insulator at all integer fillings when the band is sufficiently flat. We also show that interactions may induce effective dispersive terms strong enough to destabilize this state. These results still hold in the case of zero valley Chern number (for example, trivial side of TLG/hBN). We give an intuitive picture based on extended Wannier orbitals, and emphasize the role of the quantum geometry of the band, whose microscopic details may enhance or weaken ferromagnetism in moiré materials.

DOI: 10.1103/PhysRevLett.124.187601

Following the discovery of correlated insulators and superconductivity in magic angle twisted bilayer graphene (TBG) [1,2], a great deal of attention has been lavished on various "moiré materials." In TBG, the correlated insulator and superconductor have since been observed by other groups [3,4], leading to a wealth of new information. When the TBG is aligned with a hexagonal Boron Nitride substrate (TBG/hBN), emergent ferromagnetism and a large [5] or even quantized [6] anomalous Hall effect is observed at 3/4 filling of the conduction band. In other experiments, the moiré bands formed when ABC stacked trilayer graphene is aligned with one of the hBN (TLG/hBN) substrates display interesting strong correlation physics [7–9]. Applying a perpendicular displacement field D enables control of the bandwidth leading to a gate-tunable correlated insulator at half-filling [7]. Furthermore the sign of D controls the band topology [9–11]: the Chern number, which is equal and opposite for the two valleys, is nonzero for one sign of D and zero for the other sign. Remarkably on the topologically nontrivial side, the 1/4 filled state in the valence band shows ferromagnetism and a quantized anomalous Hall effect with Chern number 2 [9]. In yet other experiments, in twisted double bilayer graphene systems (TDBG, i.e., bilayer graphene twisted relative to another bilayer graphene to a magic angle), a spin polarized insulator [12–14] is found at half-filling of the conduction band giving way [12,13], upon doping, to a superconductor that is likely also spin polarized. Theoretically, the conduction band in TDBG also has a nonzero Chern number equal and opposite for the two valleys [10,15–17].

In this Letter, we study the physics of narrow moiré bands in the strong interaction limit; i.e., when the Coulomb interaction is much larger than the bandwidth. We focus on the moiré systems where the conduction and valence bands are separated from each other by energy gaps [18]. The spinful electrons occupy bands in two disconnected valleys (denoted + and -) such that time-reversal maps one valley to the other. As a result, the + and valleys of the active band have equal and opposite Chern number C. We call ν_T the filling fraction including the spin and valley degrees of freedom, i.e., the number of electrons per moiré unit cell in the active band. We restrict our attention to total integer fillings $\nu_T = 1, 2, 3$. We consider density-density interactions of typical strength U, and focus on the strong coupling limit $U/W \gg 1$, where W is the bandwidth of the active band. Previous papers have presented physical arguments, and supporting Hartree-Fock calculations, that the system in this limit is a spinvalley ferromagnetic insulator [10,15,19-22]. However Hartree-Fock theory typically overestimates the stability of ferromagnetic states. Thus it is important to substantiate the physical arguments for spin-valley ferromagnetism through other less biased calculations. In the context of strained graphene, Ref. [23] provided numerical evidence for a valley-polarized insulator at fractional filling. Here we present analytical arguments and numerical calculations exact diagonalization (ED) and density matrix renormalization group (DMRG)-for models pertinent to moiré materials. We show that spin-valley ferromagnetic states are stabilized in the flat-band limit even when the band is topologically trivial [20]. We provide a quantitative estimate of the stability range of the ferromagnetic states in terms of the interaction to bandwidth ratio. We also show that intervalley coherent order is always disfavored compared to ferromagnetism in the limit where the flat band is a Landau level. We emphasize that the interactions renormalize the bare (noninteracting) dispersion of the band. The strong interaction limit is thus defined as the regime where residual interactions far exceed the renormalized bandwidth.

Physical argument for ferromagnetism.—First consider the case of a topologically *trivial* band with nonzero Berry flux distribution. Such a situation arises in TLG/hBN for one sign of the displacement field D [10]. Using a Wannier basis [24,25], we can build an effective tight-binding model for the active band [20]. The Wannier functions have a finite extension which is needed to capture the Berry flux density in the band. Projecting the Coulomb interaction onto the Wannier basis leads to an on site Hubbard interaction of order U (and smaller terms between neighboring sites) but also to an intersite ferromagnetic Hund's interaction $J_F = g_s U$ [20]. The coefficient g_s depends on the overlap of Wannier densities at neighboring sites but stays finite even when $W \to 0$. In the large-U limit, the ground state has a fixed integer number ν_T of electrons at each site. The active degrees of freedom are local moments in spin-valley space. In the strict limit $W \to 0$, the only coupling that survives between these local spin-valley degrees of freedom is J_F , giving rise to a spin-valley ferromagnet [20] (see also Ref. [26]). As W increases, there will also be antiferromagnetic intersite superexchange $\alpha W^2/U$ with α a constant independent of W and U. This antiferromagnetic exchange can dominate over the intersite Hund's exchange only when $W > \sqrt{(g_s/\alpha)U}$. Thus if W/U is small enough we get a spin-valley ferromagnetic Mott insulator. In this mechanism the larger the extension of the Wannier functions, the larger the coefficient g_s , and thus the stronger the ferromagnetism.

Turning next to the case of topologically nontrivial \pm Chern bands, symmetric Wannier functions cannot be localized [24,25]; we may view this as the limit of Wannier functions with infinite extension. Intuitively, the Hund's effect will only be stronger, hence a spin-valley ferromagnetic insulator is the likely ground state at all integer fillings.

Analytical considerations.—For a perfectly flat band separated by a large gap from other bands, the effective Hamiltonian is the Coulomb interaction projected onto the active band

$$H_V = \sum_{\mathbf{q}} \delta \tilde{\rho}(\mathbf{q}) V(\mathbf{q}) \delta \tilde{\rho}(-\mathbf{q}), \tag{1}$$

where $\delta \tilde{\rho}(\mathbf{q}) = \tilde{\rho}(\mathbf{q}) - \rho_0 \delta^{(2)}(\mathbf{q})$ is the deviation of the projected density from the average density ρ_0 . The total

projected density operator $\tilde{\rho}(\mathbf{q}) = \tilde{\rho}_{+}(\mathbf{q}) + \tilde{\rho}_{-}(\mathbf{q})$ is summed over spin and valley indices, and the projected densities $\tilde{\rho}_{\pm}$ in each valley $s=\pm$ are written

$$\tilde{\rho}_s(\mathbf{q}) = \sum_{\mathbf{k},\sigma} \lambda_s(\mathbf{k} + \mathbf{q}, \mathbf{k}) c_{\mathbf{k}+\mathbf{q},\sigma s}^{\dagger} c_{\mathbf{k},\sigma s}, \tag{2}$$

where $\sigma = \uparrow, \downarrow$ is the spin index. The λ_s are valley dependent form factors which are defined in terms of the Bloch eigenstates $|u_{s,\mathbf{k}}\rangle$ through $\lambda_s(\mathbf{k}+\mathbf{q},\mathbf{k})=\langle u_{s,\mathbf{k}+\mathbf{q}}|u_{s,\mathbf{k}}\rangle$. Because of the Berry flux distribution, λ_s is a nontrivial function of \mathbf{k} and \mathbf{q} . It is readily verified that $\tilde{\rho}(-\mathbf{q})=\tilde{\rho}(\mathbf{q})^{\dagger}$ as befits the total density operator. The Hamiltonian H_V is invariant under a U(2) × U(2) rotation corresponding to independent charge and spin conservation within each valley. It is *not* SU(4) invariant in spin-valley space due to the form factors. With the further assumption that the interaction $V(\mathbf{q}) \geq 0$ for all \mathbf{q} (satisfied for Coulomb and for short range repulsive potentials), it becomes clear that H_V is positive semidefinite. Thus any state $|\psi\rangle$ that satisfies

$$\delta \tilde{\rho}(\mathbf{q})|\psi\rangle = 0 \tag{3}$$

for all q is an exact ground state.

At ν_T integer, consider the state obtained by filling up ν_T bands to form an insulator. At $\nu_T = 2$ this can be spin polarized or valley polarized. At $\nu_T = 1$, 3 this must be both spin and valley polarized. Consider a simple model that restricts the sum over momenta to the first Brillouin zone [27]; these states satisfy Eq. (3), hence they are eigenstates of H_V with eigenvalue 0. It follows that any ground state of H_V must satisfy Eq. (3) for all \mathbf{q} . The remaining question is whether the spin-valley polarized states are the unique ground states. Indeed the same argument applied to a half-filled Hubbard model in the flat band limit (zero hopping) would yield ferromagnetic ground states; but these are degenerate with all other spin configurations. In contrast in the flat Chern band, spin flips in the ferromagnetic state generically cost energy. This is well known in the idealized case of a band with uniform Berry curvature, i.e., quantum Hall ferromagnetism [28,29], where the spin stiffness ρ_s can be calculated exactly [10] and is proportional to the square of the Chern number. This suggests that these ferromagnetic states may indeed be the unique ground states for any flat Chern band.

Besides spin-valley polarized states, intervalley coherent (IVC) states are a plausible ground state candidate for moiré systems at integer filling ν_T [10,15,19,21,30] (see also Ref. [31]). To address these, it is instructive to consider a toy model where the active band is the lowest Landau level of a system with opposite magnetic fields $\pm B$ for each valley. Then the projected density operators satisfy the Girvin-MacDonald-Platzman (GMP) algebra [32] (l_B is the magnetic length):

$$[\delta \tilde{\rho}_{\pm}(\mathbf{q}), \delta \tilde{\rho}_{\pm}(\mathbf{q}')] = \pm 2i \sin\left(\frac{(\mathbf{q} \times \mathbf{q}')l_B^2}{2}\right) \delta \tilde{\rho}_{\pm}(\mathbf{q} + \mathbf{q}'). \tag{4}$$

Since the commutator has the opposite sign for the two opposite valleys, the total density satisfies

$$[\delta \tilde{\rho}(\mathbf{q}), \delta \tilde{\rho}(\mathbf{q}')] = 2i \sin\left(\frac{(\mathbf{q} \times \mathbf{q}')l_B^2}{2}\right) I^z(\mathbf{q} + \mathbf{q}'), \quad (5)$$

where $I^z(\mathbf{q}) = \delta \tilde{\rho}_+(\mathbf{q}) - \delta \tilde{\rho}_-(\mathbf{q})$ is the Fourier transform of the valley charge density. Thus in any ground state, by applying Eq. (3) to the left-hand side of Eq. (5), we find that

$$I^{z}(\mathbf{q})|\psi\rangle = 0, \quad \forall \mathbf{q} \neq 0.$$
 (6)

Thus the valley charge density cannot have fluctuations at any nonzero \mathbf{q} in a ground state. If however there is IVC order then the breaking of valley $U_v(1)$ symmetry will lead to nonzero fluctuations of $I^z(\mathbf{q})$. For instance from the expected Goldstone fluctuations of the phase of the IVC order parameter the ground state correlator

$$\langle \psi | I^z(-\mathbf{q}) I^z(\mathbf{q}) | \psi \rangle_{\mathbf{q} \to 0} = \frac{\sqrt{\kappa_v \rho_{sv}}}{2} |\mathbf{q}|.$$
 (7)

Here κ_v is the valley charge susceptibility, and ρ_{sv} is the phase stiffness of the IVC order parameter. See, e.g., Huang [33] for the analogous correlator in superfluidity. The exact result in Eq. (6) is in conflict with this expectation, therefore the IVC ordered state is not a ground state in this model. Moving away from this toy model, introducing a small bandwidth and Berry curvature fluctuations will clearly not change this result [34]. We thus expect that, as suggested by Hartree-Fock, the IVC state is disfavored relative to the spin-valley polarized states in the nearly flat band limit for generic $\pm C$ Chern bands. In what follows we will provide numerical results supporting this expectation.

Note that in realistic models, various effects are responsible for the dispersion of the active band. Besides the bare bandwidth W_{bare} of the noninteracting model, two bilinear terms of order U contribute to the overall bandwidth. The first term is the Fock term stemming from the interaction between electrons in the active band and in the fully occupied bands. The second term is the difference between H_V and its normal-ordered counterpart; it is proportional to the fluctuations of the squared form factor $|\lambda_s(\mathbf{k}+\mathbf{q},\mathbf{k})|^2$. See the Supplemental Material [37] for more details. In our analytical considerations, we considered the case where the *renormalized* bandwidth vanishes.

Exact diagonalization results for a single moiré band.— We consider the continuum momentum-space models [38] of three moiré systems (TBG/hBN [21], TDBG [10,15], TLG/hBN [10]). In our model of TBG/hBN, both top and bottom hBN substrates are aligned with TBG, in contrast to the experimental setups of Refs. [5,6] where only one hBN substrate is aligned. Unless otherwise noted, for concreteness we respectively choose the twist angles $\theta = 1.05^{\circ}$, 1.2°, and 0, and the displacement field D=0, 40, and 50 mV. The active band is the valence (TLG/hBN) or the conduction (TBG/hBN and TDBG) band and has Chern number $C = \pm 1$ (TBG/hBN), $C = \pm 2$ (TDBG), and $C = \pm 3$ (TLG/hBN) [39]. We also consider the trivial (C = 0) band obtained in TBG/hBN by rotating one hBN by a 60° angle relative to the other hBN, or in TLG/hBN by switching the sign of the displacement field D. We take the limit where the active band is separated from other bands by a gap much larger than its bandwidth. The Hamiltonian is obtained by normal ordering the projected Hamiltonian H_V of Eq. (1), where the screened Coulomb interaction takes the form

$$V(q) = U\frac{1}{q}(1 - e^{-qr_0}). (8)$$

We choose the screening length $r_0 = 5.0$ in units of the moiré lattice constant. To qualitatively address the effect of a finite dispersion of the band, we also consider the addition of a simplified kinetic term (not the realistic dispersion) which gives the active band a width W.

$$H = H_V - \frac{W_{\text{bare}}}{2} \sum_{\mathbf{k}} \cos(\mathbf{k} \cdot \mathbf{a_1} + \mathbf{k} \cdot \mathbf{a_2}) c_{\mathbf{k}}^{\dagger} c_{\mathbf{k}}, \quad (9)$$

where $\mathbf{a_1}$, $\mathbf{a_2}$ are the moiré lattice vectors. We study this model using exact diagonalization at integer filling $\nu_T = 1$, 2 ($\nu_T = 3$ is related to $\nu_T = 1$ in our model through a particle-hole transformation). We call N_s the number of moiré unit cells, and choose the aspect ratio of the finite cluster to be close to 1.

We start by investigating the nature of the ground state in the limit $W_{\text{bare}} = 0$. In spite of the band flatness, the normal ordering of the interaction induces a finite dispersion (see the Supplemental Material [37]), such that ferromagnetism is not guaranteed. Nevertheless, for $\nu_T = 1$, we find that the ground state is always fully spin and valley polarized; the resulting state has a quantum anomalous Hall effect $\sigma_{xy} = Ce^2/h$. At $\nu_T = 2$, maximal polarization of spin or valley leads to several correlated insulators all related by $U(2) \times U(2)$ symmetry in our model. For example, one with full spin polarization (but $I_z = 0$), which is a valley-Hall insulator if $C \neq 0$, and one with full valley polarization $(S_z = 0)$, with anomalous Hall effect $\sigma_{xy} = 2Ce^2/h$ [40]. Numerically, we find that these $\nu_T = 2$ polarized insulators indeed have the lowest energy in all models except for one: the C = 0 TBG/hBN. In this case, the ground state is partially polarized, but the important finite-size effects prevent us from identifying its nature.

Adding a finite bandwidth W, we find that the ferromagnetic phase survives up to $W_c \simeq 0.05U$ in some

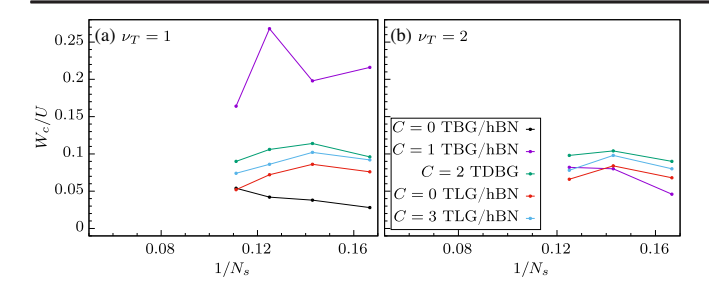


FIG. 1. Stability of the FM state in the isolated flat band upon adding a finite bandwidth $W_{\rm bare}$. The maximum value of bandwidth W_c is plotted as a function of the number of moiré unit cells N_s at filling $\nu_T=1$ and $\nu_T=2$.

models, and up to $W_c=0.2U$ in others at filling $\nu_T=1$. At $\nu_T=2$, the ferromagnet is relatively less stable, with critical values ranging from $W_c=0.04U$ to $W_c=0.1U$. The critical bandwidth is extracted from a finite-size extrapolation of exact diagonalization results which is detailed in Fig. 1.

The spin stiffness ρ_s measures the energy change from twisting the spin boundary conditions To evaluate ρ_s , we calculated the spin-wave dispersion exactly for large systems (hundreds of moiré unit cells) by restricting the calculation to the valley-polarized, $S_z = N/2 - 1$ sector. Figure 2(a) shows this dispersion in the case of the C=3 model, and displays a remarkable data collapse for $36 < N_s < 256$. Figure 2(b) illustrates the influence of the Berry curvature distribution $F(\mathbf{k})$ on the spin stiffness $[F(\mathbf{k})]$ is changed by tuning the microscopic parameters such as θ or D]. While $F(\mathbf{k})$ does not uniquely determine the spin stiffness [41], for a given model [a given color in Fig. 2(b)], larger Berry curvature fluctuations typically enhance ρ_s .

Ferromagnetism in the spin-valley Haldane model.—We now turn to DMRG calculations on infinitely long

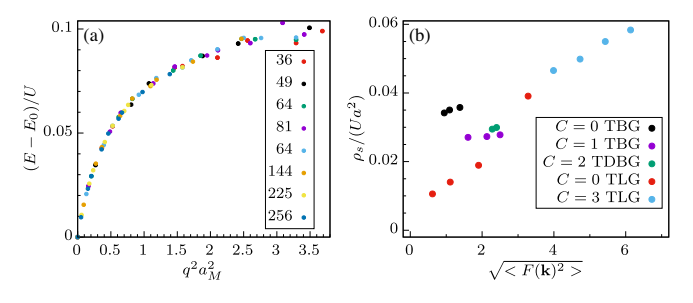


FIG. 2. Properties of low-energy spin excitations at $\nu_T=1$ and $W_{\rm bare}=0$. (a) Spin-wave dispersion around the Γ point in the $C=\pm 3$ model from exact diagonalization, for different numbers N_s of moiré unit cells. (b) Spin stiffness ρ_s as a function of the averaged squared Berry curvature $F(\mathbf{k})^2$ averaged over the Brillouin zone, evaluated from a linear fit of the spin-wave dispersion at the Γ point. a_M is the moiré lattice constant. For each model, we changed the Berry curvature distribution by adjusting the twist angle θ or the displacement field D.

cylinders, which help us circumvent the size limitations of exact diagonalization. We use a tight-binding model, which facilitates DMRG [42], but comes with an additional cost: due to the nontrivial Chern number of the active band, we must consider a two-band model. Additionally, the two-band model permits the consideration of the band gap energy scale, which we have supposed to be infinite until now. Our toy model is a tight-binding model on the honeycomb lattice based on the Haldane model [45] with on site Hubbard interaction of strength U.

$$H_{1} = -\sum_{i,j,\sigma} (t_{ij}c_{i\sigma+}^{\dagger}c_{j\sigma+} + t_{ij}^{*}c_{i\sigma-}^{\dagger}c_{j\sigma-} + \text{H.c.})$$

$$+ U \sum_{i,\sigma,\sigma',s,s'} n_{i\sigma s}n_{i\sigma's'}$$
(10)

The hopping amplitudes t_{ij} are nonzero for first and second neighbor and realize the Haldane model. We also consider third and fourth neighbor hopping. We tune these parameters to obtain a narrow conduction band with Chern number $C = \pm 1$ and $C = \pm 2$. See the Supplemental Material [37] for the details of the tight-binding model.

We numerically obtained the ground state of H_1 for infinitely long cylinders with $L_v = 2$ unit cells along the perimeter. We extracted the spin and valley polarization of the ground state for several values of U. We find that the onset of ferromagnetism U_c/W is always smaller than the band gap [see Fig. 3(c)]. Working in the valley-polarized or spin-polarized limits, we can better approach the convergence as a function of bond dimension, and simulate wider cylinders (up to $L_v = 3$). Our results are shown in Fig. 3 and confirm the ferromagnetic nature of the ground state for $U > U_c$ where $U_c \simeq 3W$ (the band gap is, respectively, $\Delta/W=6.0$ and 5.45 for the $C=\pm 1$ and $C=\pm 2$ parameters). U_c decreases with increasing system size L_v (our complementary exact diagonalization results on this model show the same trend [37]), giving us confidence that $U_c < \Delta$ in the thermodynamic limit.

Discussion.—In this Letter we have shown both analytical and numerical evidence for spin and valley

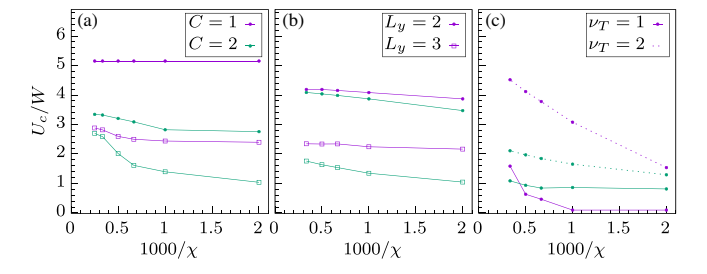


FIG. 3. Onset of ferromagnetism in the C=1, 2 Honeycomb model Eq. (10), extracted from DMRG on cylinders of perimeter L_y , as a function of the bond dimension χ . (a) Valley-polarized model, $\nu_T=1$. (b) Spin-polarized model, $\nu_T=1$. (c) Full spin and valley model at $\nu_T=1$, 2, limited to $L_y=2$.

polarization in nearly flat bands, which emerge in several graphene moiré superlattices. Our results demonstrate a valley and spin polarized quantum anomalous Hall insulator at $\nu_T = 1$ or $\nu_T = 3$. At $\nu_T = 2$, a spin-polarized valley Hall insulator and a valley-polarized quantum anomalous Hall insulator are both possible. Indeed recent experiments have already observed signatures for spin polarization in twisted double bilayer graphene and anomalous Hall effect in TBG/hBN [5] and TLG/hBN [9].

The phenomenon we described is reminiscent of quantum Hall ferromagnetism, but there are important differences. Most naively, the finite bandwidth may destroy ferromagnetism, and we have quantitatively evaluated the position of this transition. Further, flat-band ferromagnetism appears even when the Chern number is zero, due to the nonzero Berry flux. Deviating from the Landau level situation through large Berry curvature fluctuations has two opposite effects, which, respectively, destabilize and stabilize ferromagnetism: it may increase the strength of interaction-induced dispersive terms, but it may also enhance the spin stiffness. A natural future direction is to study the possibility of fractional quantum Hall effect from similar spontaneous time reversal breaking at fractional filling.

We are thankful to Yin-Chen He and Kun Yang for insightful discussions. We thank Eslam Khalaf for pointing out an error in the initial version of this manuscript. DMRG calculations were performed using the TeNPy Library (version 0.4.0) [46]. This work was supported by NSF Grant No. DMR-1911666, and partially through a Simons Investigator Award from the Simons Foundation to Senthil Todadri. C. R. is supported by the Marie Sklodowska-Curie program under EC Grant Agreement No. 751859. Part of this work was performed during a visit of C. R. and T. S. at Aspen Center for Physics, which is supported by National Science Foundation Grant No. PHY-1607611. C. R. performed the ED simulations, Z.D. performed the DMRG simulations. Y. H. Z. provided the momentum space and lattice models. C. R., Y. H. Z., and T. S. supervised the work of Z. D. All authors contributed to the discussions and analysis of results.

- [1] Y. Cao, V. Fatemi, A. Demir, S. Fang, S. L. Tomarken, J. Y. Luo, J. D. Sanchez-Yamagishi, K. Watanabe, T. Taniguchi, E. Kaxiras *et al.*, Nature (London) **556**, 80 (2018).
- [2] Y. Cao, V. Fatemi, S. Fang, K. Watanabe, T. Taniguchi, E. Kaxiras, and P. Jarillo-Herrero, Nature (London) 556, 43 (2018).
- [3] M. Yankowitz, S. Chen, H. Polshyn, Y. Zhang, K. Watanabe, T. Taniguchi, D. Graf, A. F. Young, and C. R. Dean, Science 363, 1059 (2019).
- [4] X. Lu, P. Stepanov, W. Yang, M. Xie, M. A. Aamir, I. Das, C. Urgell, K. Watanabe, T. Taniguchi, G. Zhang,

- A. Bachtold, A. H. MacDonald, and D. K. Efetov, Nature (London) **574**, 653 (2019).
- [5] A. L. Sharpe, E. J. Fox, A. W. Barnard, J. Finney, K. Watanabe, T. Taniguchi, M. A. Kastner, and D. Goldhaber-Gordon, Science 365, 605 (2019).
- [6] M. Serlin, C. L. Tschirhart, H. Polshyn, Y. Zhang, J. Zhu, K. Watanabe, T. Taniguchi, L. Balents, and A. F. Young, Science 367, 900 (2020).
- [7] G. Chen, L. Jiang, S. Wu, B. Lyu, H. Li, B. L. Chittari, K. Watanabe, T. Taniguchi, Z. Shi, J. Jung, Y. Zhang, and F. Wang, Nat. Phys. 15, 237 (2019).
- [8] G. Chen, A. L. Sharpe, P. Gallagher, I. T. Rosen, E. Fox, L. Jiang, B. Lyu, H. Li, K. Watanabe, T. Taniguchi, J. Jung, Z. Shi, D. Goldhaber-Gordon, Y. Zhang, and F. Wang, Nature (London) 572, 215 (2019).
- [9] G. Chen, A. L. Sharpe, E. J. Fox, Y.-H. Zhang, S. Wang, L. Jiang, B. Lyu, H. Li, K. Watanabe, T. Taniguchi, Z. Shi, T. Senthil, D. Goldhaber-Gordon, Y. Zhang, and F. Wang, Nature (London) 579, 56 (2020).
- [10] Y.-H. Zhang, D. Mao, Y. Cao, P. Jarillo-Herrero, and T. Senthil, Phys. Rev. B 99, 075127 (2019).
- [11] B. L. Chittari, G. Chen, Y. Zhang, F. Wang, and J. Jung, Phys. Rev. Lett. 122, 016401 (2019).
- [12] X. Liu, Z. Hao, E. Khalaf, J. Y. Lee, K. Watanabe, T. Taniguchi, A. Vishwanath, and P. Kim, arXiv:1903.08130.
- [13] C. Shen, N. Li, S. Wang, Y. Zhao, J. Tang, J. Liu, J. Tian, Y. Chu, K. Watanabe, T. Taniguchi, R. Yang, Z. Y. Meng, D. Shi, and G. Zhang, Nat. Phys. (2020), https://www.nature.com/articles/s41567-020-0825-9.
- [14] Y. Cao, D. Rodan-Legrain, O. Rubies-Bigordà, J. M. Park, K. Watanabe, T. Taniguchi, and P. Jarillo-Herrero, arXiv: 1903.08596.
- [15] J. Y. Lee, E. Khalaf, S. Liu, X. Liu, Z. Hao, P. Kim, and A. Vishwanath, Nat. Commun. 10, 5333 (2019).
- [16] M. Koshino, Phys. Rev. B 99, 235406 (2019).
- [17] J. Liu and X. Dai, Phys. Rev. X 9, 031021 (2019).
- [18] This is not the case in the original TBG where Dirac points connect conduction and valence bands.
- [19] N. Bultinck, S. Chatterjee, and M.P. Zaletel, arXiv: 1901.08110.
- [20] Y.-H. Zhang and T. Senthil, Phys. Rev. B **99**, 205150 (2019).
- [21] Y.-H. Zhang, D. Mao, and T. Senthil, Phys. Rev. Research 1, 033126 (2019).
- [22] M. Xie and A. H. MacDonald, Phys. Rev. Lett. 124, 097601 (2020).
- [23] P. Ghaemi, J. Cayssol, D. N. Sheng, and A. Vishwanath, Phys. Rev. Lett. 108, 266801 (2012).
- [24] C. Brouder, G. Panati, M. Calandra, C. Mourougane, and N. Marzari, Phys. Rev. Lett. **98**, 046402 (2007).
- [25] N. Marzari, A. A. Mostofi, J. R. Yates, I. Souza, and D. Vanderbilt, Rev. Mod. Phys. 84, 1419 (2012).
- [26] J. Kang and O. Vafek, Phys. Rev. Lett. 122, 246401 (2019).
- [27] Though this is a good approximation [given the rapid decay of $\lambda_s(\mathbf{k}+\mathbf{q},\mathbf{k})$], our numerical results do not invoke this restriction.
- [28] S. L. Sondhi, A. Karlhede, S. A. Kivelson, and E. H. Rezayi, Phys. Rev. B 47, 16419 (1993).
- [29] Z. F. Ezawa and G. Tsitsishvili, Rep. Prog. Phys. 72, 086502 (2009).

- [30] J. Jung, A. M. DaSilva, A. H. MacDonald, and S. Adam, Nat. Commun. 6, 6308 (2015).
- [31] H. C. Po, L. Zou, A. Vishwanath, and T. Senthil, Phys. Rev. X **8**, 031089 (2018).
- [32] S. M. Girvin, A. H. MacDonald, and P. M. Platzman, Phys. Rev. B 33, 2481 (1986).
- [33] K. Huang, *Statistical Mechanics*, 2nd ed. (John Wiley and Sons, Inc., 1987).
- [34] In a generic Chern band, the GMP algebra is approximated in the $\mathbf{q} \to 0$ limit [35,36], and Eq. (6) still holds in this limit.
- [35] S. A. Parameswaran, R. Roy, and S. L. Sondhi, C.R. Phys. 14, 816 (2013).
- [36] C. Repellin, T. Neupert, Z. Papić, and N. Regnault, Phys. Rev. B 90, 045114 (2014).
- [37] See the Supplemental Material at http://link.aps.org/supplemental/10.1103/PhysRevLett.124.187601 for more details on the renormalization of the bare bandwidth by interactions, and additional numerical data.
- [38] R. Bistritzer and A. H. MacDonald, Proc. Natl. Acad. Sci. U.S.A. 108, 12233 (2011).
- [39] In TLG/hBN, a quantized anomalous Hall effect was in fact observed at C=2 [9]. Here, we use the continuum

- noninteracting model which predicts a Chern $C=\pm 3$ band. A scenario involving interactions and supported by Hartree-Fock calculations was proposed in Ref. [9] to explain this discrepancy.
- [40] Including the weak intervalley Hund's interaction would break the $U(2) \times U(2)$ symmetry and lift the degeneracy between these two states.
- [41] Even in the case of uniform Berry curvature, the real part of the quantum geometric tensor also enters the expression of ρ_s [10].
- [42] While it is in principle possible to perform DMRG using a hybrid momentum-real space basis [43,44], it comes with the cost of longer-range interactions and more complex algorithms.
- [43] J. Motruk, M. P. Zaletel, R. S. K. Mong, and F. Pollmann, Phys. Rev. B 93, 155139 (2016).
- [44] G. Ehlers, S. R. White, and R. M. Noack, Phys. Rev. B 95, 125125 (2017).
- [45] F. D. M. Haldane, Phys. Rev. Lett. 61, 2015 (1988).
- [46] J. Hauschild and F. Pollmann, SciPost Phys. Lect. Notes, 5 (2018), code available from https://scipost.org/ SciPostPhysLectNotes.5.